Validation of CATHENA for Flow Oscillation in Frequency Domain

X. Huang and G. Waddington
Code Assessment and Validation, Thermalhydraulics Branch
Atomic Energy of Canada Limited, Chalk River, Ontario, Canada K0J 1J0
(huangxi@aecl.ca)

Abstract

This paper reports on the validation of CATHENA for flow oscillations. The time-dependent results from the flow oscillation experiment and from the CATHENA simulation were detrended and then transferred into the frequency domain using discrete Fourier transform for comparison. Sensitivities of the modelling options and impacts of uncertainties from the code inputs on the predicted key parameter were also assessed in the frequency domain. The reported work demonstrates that the accuracy of CATHENA in predicting flow oscillation frequencies and amplitudes can be assessed precisely in the frequency domain.

1. Introduction

Flow instability and oscillation has been a matter of investigations for many years. In nuclear technology, it is of increasing importance because it can induce mechanical vibration and thermal fatigue, cause system control problems, and result in changes to local heat transfer rates potentially leading to fuel bundle sheath and pipe wall surface temperature excursions. It is also relevant to chemical and mechanical engineering. Flow instability and oscillation in a CANDU reactor are generally simulated by CATHENA, a Canadian thermalhydraulics network code for nuclear reactor analyses.

Validation of CATHENA is mostly conducted by comparing the predicted and measured key output parameters in the time domain. In the CATHENA validation for the flow oscillation phenomenon, comparison of the predicted and measured key output parameters in the time domain provides an assessment of the CATHENA code's capability in capturing the peaks and troughs of the key output parameters (e.g. the system pressures and sheath temperatures) during the experiment transients; this information is important for the system control and fuel bundle safety of a reactor. On the other hand, assessment of the CATHENA code's capability in capturing the oscillation frequency and amplitude is also important for the mechanical vibration and thermal fatigue analysis of a reactor; such an assessment can be achieved by comparing the predicted and measured key output parameters (oscillation frequency and amplitude) in the frequency domain.

This paper describes a CATHENA validation exercise for the flow oscillation phenomenon in the frequency domain, using data from a depressurization-induced flow oscillation experiment (F8903) performed in a CANDU-typical experimental facility (RD-14M). This paper introduces a technical background for applying the "frequency domain" method to CATHENA validation, including sensitivity and uncertainty analyses.

2. Experimental Set-Up and CATHENA Idealization

The RD-14M facility is a full-elevation scaled thermalhydraulic test facility possessing most of the key components of a CANDU primary heat transport system. A simplified schematic of the facility is shown in Figure 1 (left). The RD-14M design incorporates the basic "figure-of-eight" geometry of a CANDU reactor with 5 horizontal fuel channels per pass. The ten full-length channels are complete with end-fitting simulators. Each channel contains a 6.0 m long heated section comprised of 7 indirectly electrically heated fuel element simulators (FESs) as shown in Figure 1 (right).

Prior to RD-14M flow oscillation Test F8903, the loop was emptied, filled, and degassed. All instrument readings were checked and adjusted. The loop was warmed at low power and low pump speeds. The heated section powers and pump speeds were then adjusted to bring the loop to the desired single-phase steady-state conditions. After the steady state had been reached, the outputs from all the instruments were scanned and printed as a final check and data acquisition began. Steam quality was then induced into the primary loop through a series of depressurization steps. The surge tank was switched off-line and on-line a number of times to investigate the effect of surge tank isolation on flow oscillations. The heated-section powers were held constant. Transient experimental data were collected at one-second intervals. The sequences of events during the experiment are listed in Table 1.

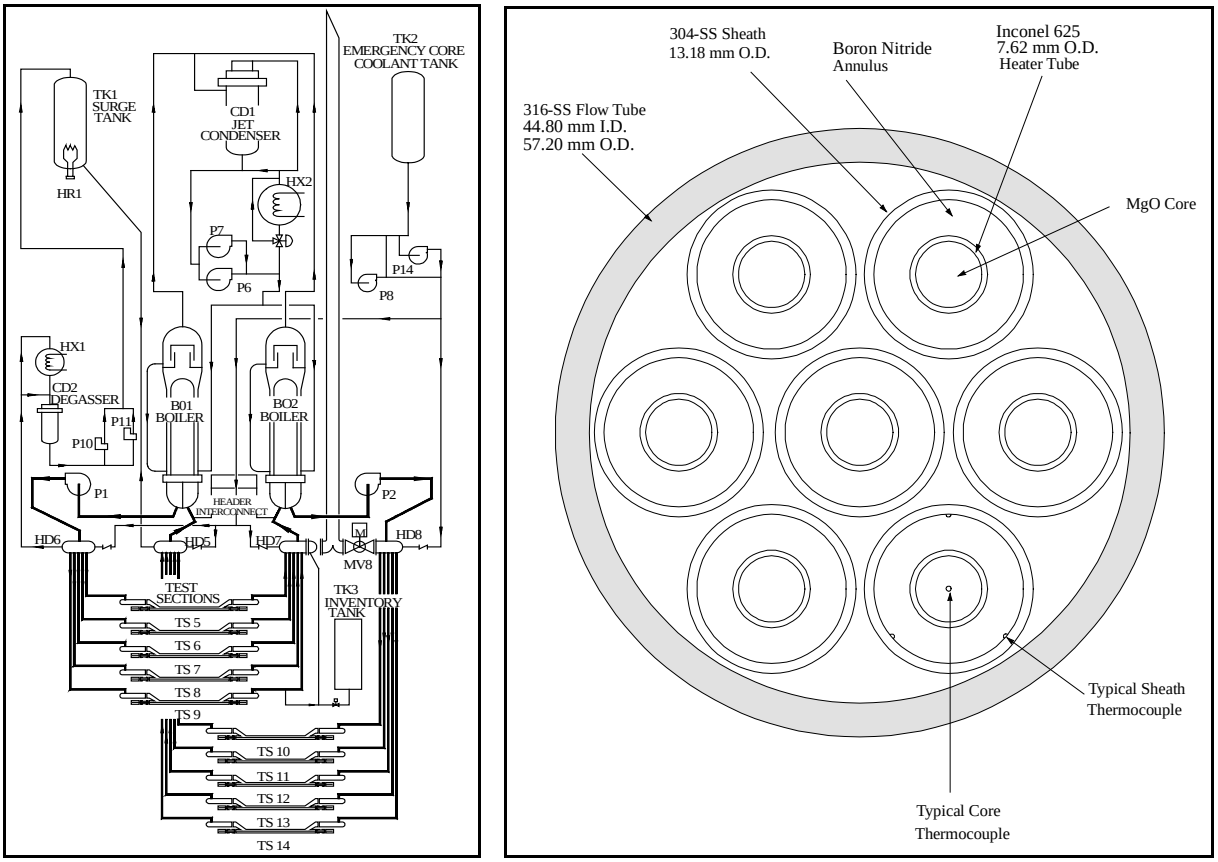

Figure 1: RD-14M Loop Schematic (left) and Cross-section of Heated Channel (right)

Table 1: Timing of Significant Events in RD-14M Test F8903

Time (s)	Event
0	Data gathering began
180	Scans stopped and restarted
240	Primary pressure reduced from 10 MPa(g) to 9.7 MPa(g)
449	Surge tank isolated
544	Surge tank on line
660	Primary pressure reduced from 9.7 MPa(g) to 9.4 MPa(g)
866	Surge tank isolated
1101	Surge tank on line
1380	Primary pressure reduced from 9.4 to 9.0 MPa(g)
1608	Surge tank isolated
1702	Surge tank on line
1920	Primary pressure reduced from 9.0 to 8.7 MPa(g)
2059	Surge tank isolated
2173	Surge tank on line
2340	Primary pressure reduced from 8.7 to 8.5 MPa(g)
2548	Surge tank isolated
2675	Surge tank on line
2820	Scans stopped

Figure 2 shows the CATHENA idealization used to model the primary-side piping (left, only one pass is shown for clarity), and the secondary side (right). The primary side consists of all piping connecting the headers, heated sections, steam generators, pumps, and pressurizer (surge tank). The idealization includes a tank model to simulate the pressurizer with its 100 kW heater and venting line. In the simulation, venting for the depressurization and the heating operation for maintaining the surge tank pressure, are controlled by system control models. The heating power is proportional to the positive difference between the set-up pressures and the inlet header HD5 pressure. A 'RESERVOIR' model was linked to the end of the surge line to apply the boundary conditions to the primary system during the initial steady-state simulation.

3. Transfer Time-Series Data to Frequency Domain

For comparison, the experimentally measured and CATHENA predicted data are transferred from the time domain to the frequency domain. This transfer is achieved by (1) detrending the time-series data; then (2) performing a Fourier transform on the detrended data.

Detrending is basically a statistical or mathematical operation of removing the trend from the time-series data, and is often applied to remove a feature thought to distort or obscure the relationships of interest. Many alternative methods are available for detrending. The detrending method applied in this study is to remove the trend calculated by the locally weighted regression of the original time-series data. The number of data points applied in the regression was selected to be 10% of the total number of the sampling data points. To obtain a high resolution in the frequency domain, the sampling interval of the time-series data needs to be sufficiently fine and the sampling time of the time-series data should be sufficiently long, because according to the sampling law the maximum frequency that can be detected is

the Nyquist frequency (f_n), which is half of the sampling rate, and the achievable frequency resolution is f_n/N (N is the total number of sampling data).

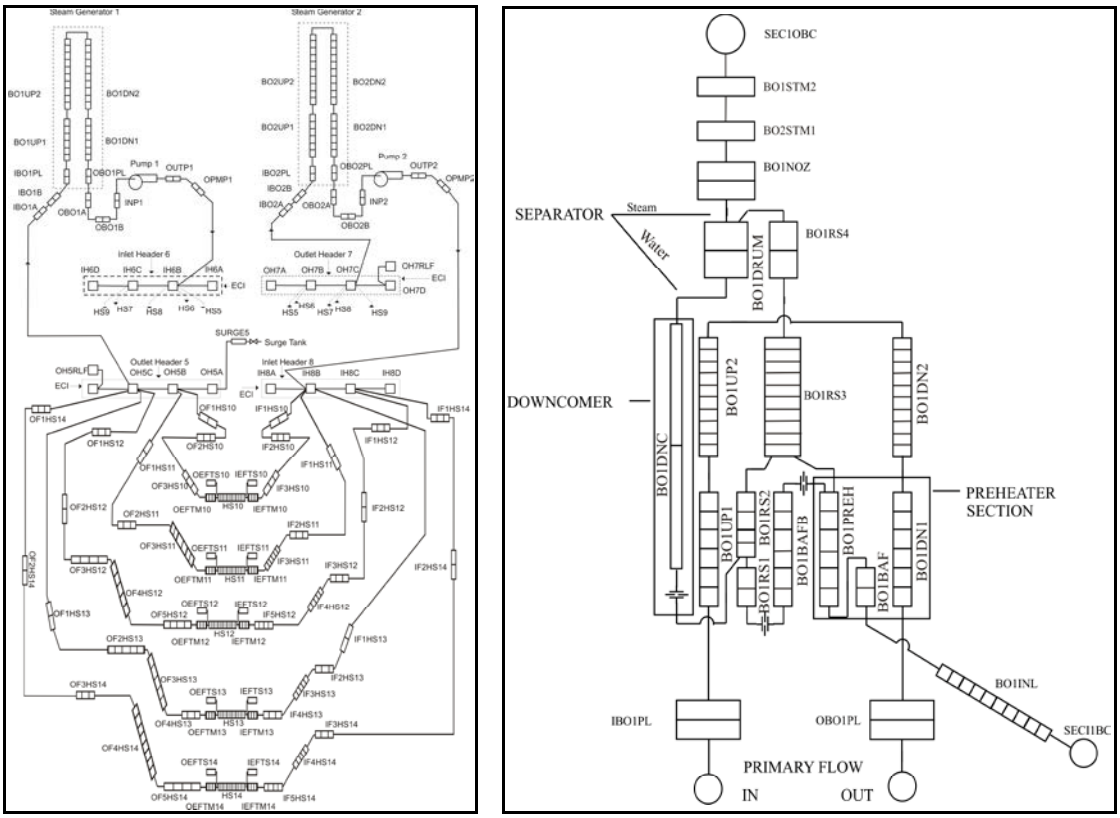

Figure 2: CATHENA Idealization of the RD-14M Primary Side (left) and Secondary Side (right)

The Discrete Fourier Transform (DFT) converts discrete data from a time wave into a frequency spectrum. Using the DFT implies that the finite segment that is analysed is one period of an infinitely extended periodic signal. The formula for the DFT applied is:

$$F(n) = \sum_{k=0}^{N-1} x(k) e^{\frac{-j2\pi kn}{N}}$$

In this study, the detrending was performed using a SigmaPlot® function "lowess", and the DFT of the detrended data was performed using the software "Spectra 1.13" from the Nuhertz Technologies, LLC.

4. CATHENA Simulation Results and Discussion

The simulations were performed on a Windows XP cluster server. Each transient simulation starts from a steady-state run. After a steady-state condition has been reached, a transient run is performed and the time-dependent output parameters are saved to output files for post-processing and data transferring. For brevity, the results for only one key output parameter,

i.e. the flow rates at the primary pump outlets, are presented below. Discussions are focused mainly on the frequency domain results.

4.1 Base Case Simulation

The experimentally measured and CATHENA calculated volumetric loop flow rates at the outlets of the PHT pumps 1 and 2 are plotted in Figure 3 for the duration of the transient. The two pump flow rates have the same trends and oscillations; therefore the following discussions are applicable to both loops in the test. CATHENA captured the general trends and flow oscillations in the pump flows for both loops.

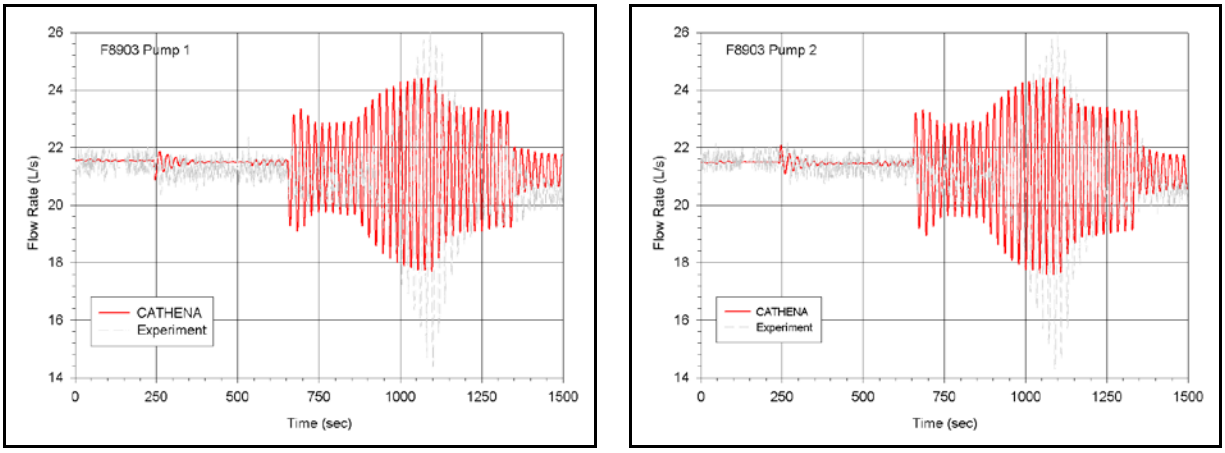

Figure 3: Measured and CATHENA Predicted Outlet Flow Rates of Pump 1 and Pump 2

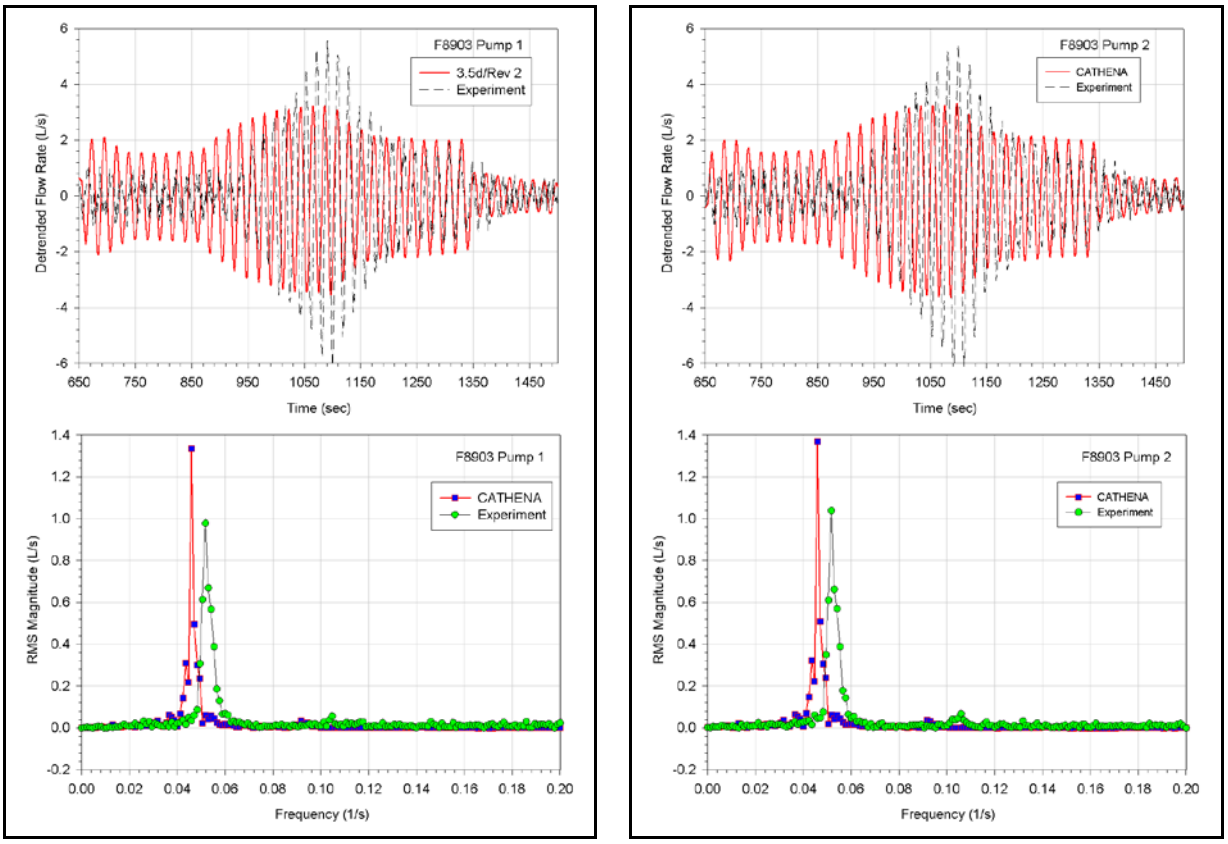

Figure 4: Measured and Predicted Pump 1 and 2 Detrended Loop Flow Rates and Periodiagrams

Since flow oscillations were observed mainly after 650 s, the detrended experimentally measured and CATHENA calculated volumetric flow rates at the pump 1 and 2 outlets for the time period from 650 s to 1500 s are plotted in Figure 4 (top), along with the corresponding periodiagrams (bottom) of the detrended flow rate oscillations. The periodiagram data in the frequency domain was discretized with frequency intervals of 1/850 (or 0.0011765) Hz. Figure 4 (bottom) shows that both the measured and predicted flow oscillations have a strong dominant harmonic around 0.05 Hz. CATHENA slightly underestimates the dominant frequency (0.0459 vs. 0.0518 Hz), and overestimates the dominant amplitude (approximately 1.35 vs. 1.05 L/s) of the flow oscillation.

4.2 Sensitivity Analysis

The objective of the sensitivity analysis is to assess one-by-one the impacts of changes in the CATHENA model on the simulation results. In the sensitivity analysis, the effects of spatial nodalization, time step size (the maximum time step), and pump heating, on the predicted key output parameters, are assessed. For brevity, sensitivity analysis results for only the maximum time step size and pump heating are presented and discussed.

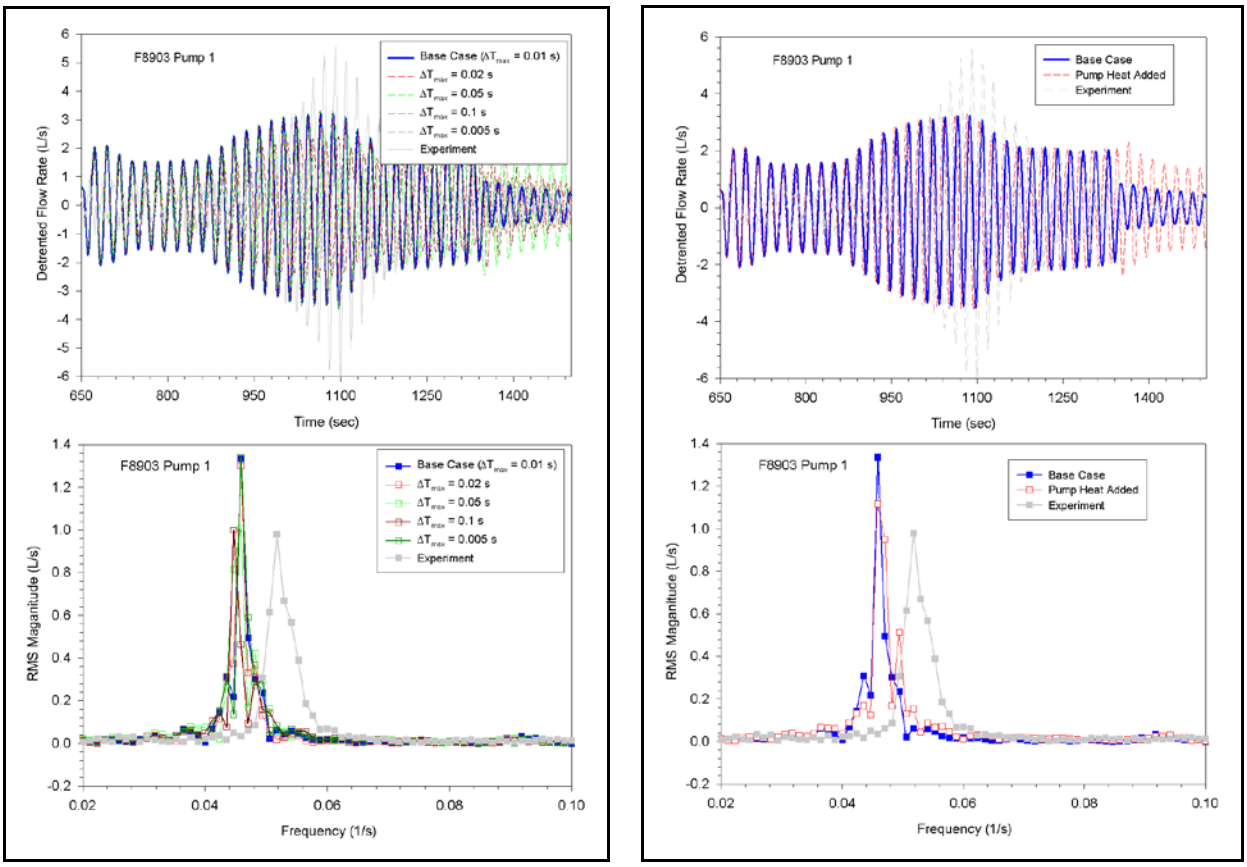

Figure 5: Sensitivity of Predicted Pump 1 Outlet Flow Rate to Time Step Size and Pump Heat

Table 2: Sensitivities of Modelling Options on Predicted Pump 1 Outlet Flow

	Dominant Frequency (Hz)	Dominant Amplitude (L/s)
Experiment	0.0518	0.979
Simulation Cases		
Base Case (Max TS = 0.01 s, No Pump Heat)	0.0459	1.335
Max TS = 0.1 s	0.0447	0.999
Max TS = 0.05 s	0.0459	1.009
Max TS = 0.02 s	0.0459	1.302
Max TS = 0.005 s	0.0459	1.340
Pump Heat Considered	0.0459	1.116

The effects of time step size and pump heat, on the predicted Pump 1 outlet flow rate, are shown in Figure 5 and summarized in Table 2. Note that increasing the maximum time step size by a factor of less than 10, decreasing the maximum time step size by a factor of 2, or considering pump heat in the idealization does not change the predicted dominant frequency. Sensitivity impacts of the modelling options investigated on the predicted dominant amplitude are less than 0.226 L/s. Increasing or decreasing the maximum time step size by a factor of 2 does not significantly affect the prediction of either the dominant frequency or amplitude

(Figure 5, bottom left; and Table 2), indicating that the selected maximum time step size of 0.01 s is appropriate for reaching a temporally converged solution.

4.3 Uncertainty Analysis

An integrated uncertainty analysis was performed following the GRS (Gesellschaft für Anlagen- und Reaktorsicherheit) method of order statistics [1]. Applying Wilks' formula [2], a total of 93 CATHENA MOD-3.5d/Rev 2 simulation runs were conducted for the uncertainty analysis to ensure with 95% confidence that the smallest and the largest of the predicted key output parameters (RMS magnitudes of oscillation amplitudes in frequency domain) bound at least 95% of the key output parameter population distribution. A total of 96 code inputs were identified as being potentially influential to the prediction of the loop flow rates. In each uncertainty analysis simulation, these 96 input parameters were randomly perturbed using simple random sampling of their assumed probability distribution function (listed in Table 3). These code inputs can be divided into two categories: experimentally measured parameters used in the CATHENA input file as boundary or initial conditions, and correlations and models embedded in the CATHENA code.

Figure 6 (left) shows the 93 detrended pump 1 flow rates and the corresponding periodiagram for the time period from 650 s to 1500 s. Also shown are the corresponding periodiagrams from the base case (or best estimate) simulation, and from the experiment. The perturbations of the code inputs have a larger impact on the predicted dominant amplitudes than on the predicted dominant frequency (see also Figure 6 top right). The maximum and minimum values of all 93 amplitudes of the periodiagram are shown in Figure 6 (bottom right); these are the 95%/95% upper and lower tolerance limits for the predicted flow oscillation frequency and amplitude. Note that the lower tolerance limits of the predicted dominant amplitudes are almost zero, indicating that no significant oscillation was predicted in simulations with certain combinations of the code input (boundary condition) values.

Table 3: List of Code Inputs and Their Uncertainties for Uncertainty Analysis

Parameter Category	Parameter Description	Distribution	Std. Dev. (σ)	Bias (ε)
Code Inputs from CATHENA Boundary & Initial Conditions	Initial System Pressure (in Surge Tank)	Normal	0.05 MPa	0.0
	Secondary Side Pressure (in Boiler Drum)	Normal	0.025 MPa	0.0
	Feedwater Temperature	Normal	2.0 °C	0.0
	Feedwater Mass Flow	Normal	1.25%	0.0
	Heated Section Power (PS1~PS4)	Normal	4.7%	0.0
	Primary Pump 1 Speed	Normal	1%	0.0
	Primary Pump 2 Speed	Normal	1%	0.0
Code Inputs from CATHENA Correlations	Two-Phase Friction Multiplier (HTFS) τ^*	Normal	23%	0.0
	Freidel Two-Phase Flow Multipliers τ^* (Skin Friction & Minor Loss, Crept)	Nomal	4.34%	-0.16%
	Colebrook-White Wall Friction Factor $f(\varepsilon \neq 0)$	Normal	15%	0.0
	C_{si} (0.8004)	Uniform	Range: 0.3162 to 2.8228	
	$J_{f,min}$ (0.085)	Uniform	Range: 0.04 to 0.2	
	C_f (0.2)	Uniform	Range: 0.15 to 0.25	
	V_r^c (a=2.6)	Uniform	Range: 2.6 to 11.78	
	V_r^c (b=-0.2)	Uniform	Range: -0.333 to –0.2	
	Interphase HTC (bubbly) $\lambda_{ki,b}$	Normal	20%	0.0

	Interphase HTC (slug/churn) $\lambda_{ki,s}$	Normal	20%	0.0
	Interphase HTC (droplet) $\lambda_{ki,d}$	Normal	20%	0.0
	Interphase HTC (vapour) $\lambda_{gi,1}$	Normal	20%	0.0
	Interphase HTC (subcooled steam) $\lambda_{qi,2}$	Normal	20%	0.0
	Interphase HTC (superheated liquid) $\lambda_{fi,1}$	Normal	20%	0.0
	Interphase HTC (stratified) $\lambda_{fi,2}$	Normal	20%	0.0
	Interphase HTC (annular) λ_{fi}^{TURB}	Normal	20%	0.0
	Interphase HTC (piston) λ_{fi}^{MIN}	Normal	20%	0.0
	Convection & Nucleate Boiling Heat Transfer h^{i}_{LC}, h_{SP}, h_{ct}, h_{NB} (Modified Chen)	Normal	12.9%	0.0
	Onset of Nucleate Boiling, T_{ONB}	Uniform	Range: 0 to 2 °C	
	Onset of Significant Void (Saha-Zuber) q''_{OSV}	Normal	10%	0.0
	Onset of Siginificant Void (Saha-Zuber, Crept) q''_{OSV}	Normal	4.69%	0.0
	Convection & Nucleate Boiling Heat Transfer h^{i}_{LC}, h_{SP}, h_{ct}, h_{NB} (Modified Chen)	Normal	12.9%	0.0
	Onset of Nucleate Boiling, T_{ONB}	Uniform	Range: 0 to 2 °C	
	Onset of Significant Void (Saha-Zuber) q''_{OSV}	Normal	10%	0.0
	Onset of Siginificant Void (Saha-Zuber, Crept) q''_{OSV}	Normal	4.69%	0.0
	CHF (Groeneveld-Leung table) q''^{a}_{CHF}	Normal	7.82%	0.69%
	Transition Boiling (Bjornard-Griffith) T_w	Normal	8.1%	0.0
	Stable Film Boiling (Wall-Superheat PDO Table T_{sup})	Normal	10.63%	-0.03%
	Groeneveld-Stewart, T_{wet}	Normal	8.1%	2.6%
	Zuber-Griffith, q''_{CHF}	Normal	12.5%	0.0
	Single Phase, Pump Head H* (α=0)	Normal	0.02	-0.002
	Two-Phase Pump Head H* (α>0)	Normal	0.296	-0.003
	Pump Functions, Multiplier Void, α_g	Normal	0.1	0.1
	Interphase Apparent Density ρ_{AP}	Normal	5.0%	0.0
	Interphase Friction Factor (bubbly) $f_{i,b}$	Normal	20%	0.0
	Interphase Friction Factor (slug) $f_{i,ss}$	Normal	22%	0.0
	Interphase Friction Factor (Horizontal Stratified) $f_{i,s}$	Normal	15%	0.0
	Interphase Friction Factor (Horizontal Stratified) $f_{i,w}$	Uniform	Range: 0.0 to 2.0	
Minor Losses of Channels	Minor Losses of 10 Test Sections HS5~HS14	Normal	9%	0.0
Material Properties	Stainless Steel Thermal Conductivity	Normal	2%	0.0
	Stainless Steel Thermal Diffusivity	Normal	5%	0.0
	MgO Thermal Conductivity (a table of 9 entries)	Uniform	Range: 0.94 to 1.09	
	MgO Thermal Diffusivity (a table of 9 entries)	Uniform	Range: 0.99 to 1.04	
	BN Thermal Conductivity (a table of 10 entries)	Uniform	Range: 0.93 to 1.12	
	BN Thermal Diffusivity (a table of 10 entries)	Uniform	Range: 0.99 to 1.06	

In the frequency domain, the code bias (ε) is defined as the difference between predicted best estimate (X_{be}) and measured (X_{exp}) RMS magnitudes or frequencies of the oscillation. The uncertainty limits of the code bias estimation can be estimated by combining uncertainties from both simulations and experimental measurements as ($\varepsilon-\Delta\varepsilon^{-}$, $\varepsilon+\Delta\varepsilon^{+}$), where

$$\Delta\varepsilon^{+} = \sqrt{\left(X_{\max} - X_{be}\right)^2 + \left(1.96\,\sigma_e\right)^2}\ ,\ \Delta\varepsilon^{-} = \sqrt{\left(X_{be} - X_{\min}\right)^2 + \left(1.96\,\sigma_e\right)^2}\ ,$$

and σ_e is the measurement uncertainty.

The calculated code biases and their uncertainty limits of the predicted dominant amplitude and frequency of the pump 1 flow oscillation for the time period from 650 s to 1500 s are summarized in Table 4.

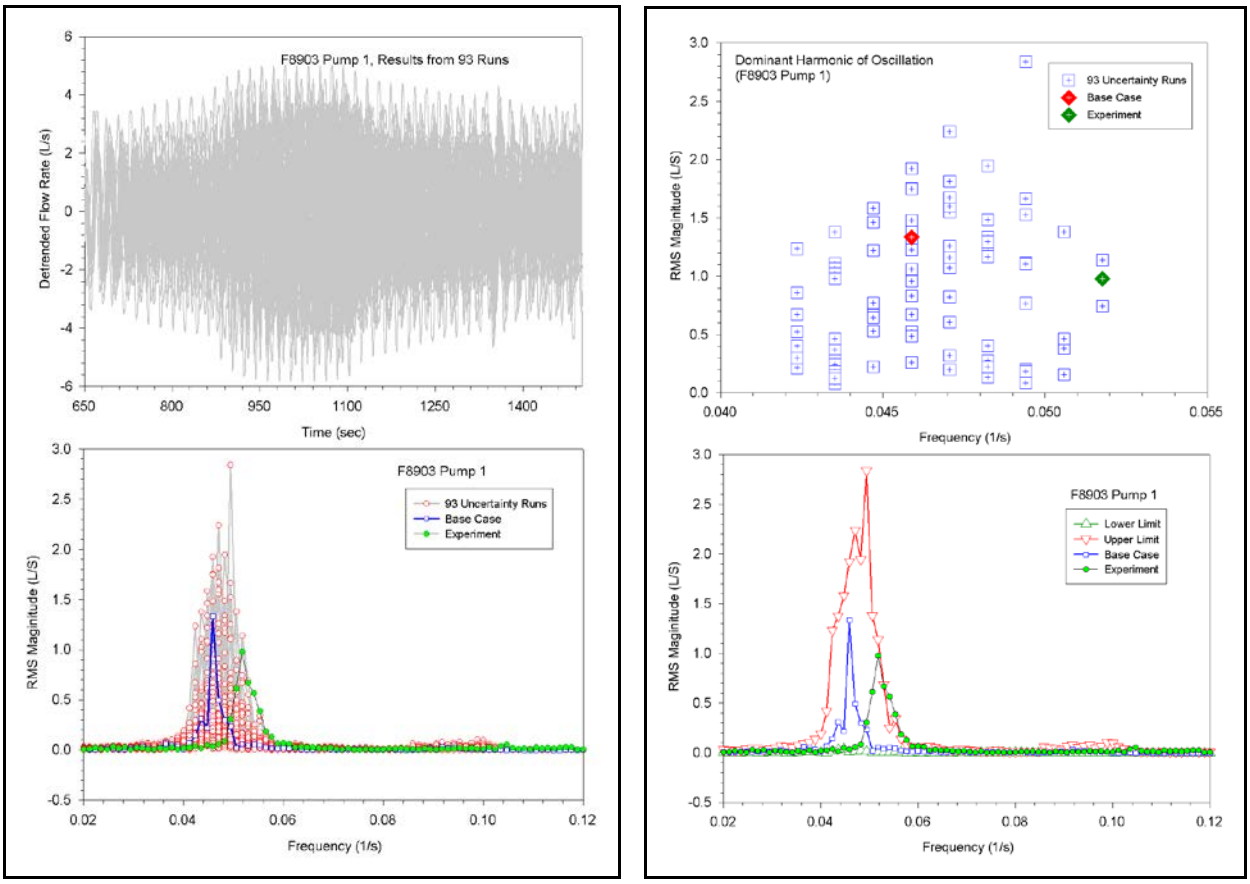

Figure 6: Impact of Code Input Uncertainties on Predicted Pump 1 Outlet Flow Rate

Table 4: CATHENA Code Biases for Dominant Amplitude and Frequency

	Dominant Frequency (Hz)	Dominant Amplitude (L/s)
Experiment	0.0518	0.979
Base Case (X_{be})	0.0459	1.335
95%/95% Upper Tolerance Limit (X_{max})	0.0518	2.841
95%/95% Lower Tolerance Limit (X_{min})	0.0424	0.084
Code Bias (ε)	-0.0059	0.356
Measurement Uncertainty (σ_e)	0.0011765	0.01
Upper Uncertainty Limit ($\Delta\varepsilon^+$)	0.006335	1.506
Lower Uncertainty Limit ($\Delta\varepsilon^-$)	0.009679	1.251

5. Conclusions

This paper presents a CATHENA validation exercise for flow oscillations in the frequency domain, using data from a depressurization-induced flow oscillation experiment (F8903) performed in a CANDU-typical experimental facility (RD-14M). The main conclusions drawn from this work are:

- CATHENA validation is generally conducted in the time domain; however, validation in the frequency domain is a better way to assess the code's capability to capture the amplitudes and frequencies of flow oscillations. The demonstrated base case validation result shows that in the frequency domain, CATHENA underestimates the dominant frequency by 11.4% and overestimated the dominant amplitude by 36%.
- The two additional steps to conduct a validation exercise in the frequency domain are: 1) detrending the time-series data; and 2) the Fourier transform of the detrended data into periodiagrams. Frequency resolutions of the periodiagrams in the frequency domain are determined by the sampling rates of the time-series data. A higher sampling rate of the time-series data means a higher frequency resolution of the periodiagrams (*Nyquist sampling law*).
- Sensitivity and uncertainty analyses for the validation exercise can also be performed in the frequency domain following the same approach as for the time domain. Due to the relatively low resolution (0.0011765 Hz) in the frequency domain, the sensitivity effects and code biases are calculated for only the dominant amplitudes and frequencies.

6. References

[1] H.G. Glaeser, "Uncertainty Evaluation of Thermal-Hydraulic Code Results", Int. Meeting on 'Best Estimate' Methods in Nuclear Installation Safety Analysis (BE 2000), Washington D.C., 2000 November.

[2] L. Sachs, "Applied Statistics", Second edition, Springer Verlag, 1984.